Exploring implication of variation in biochar production on geotechnical properties of soil

Article

Accepted Version

Exploring implication of variation in biochar production on geotechnical properties of soil

Suriya Prakash Ganesan, Sanandam Bordoloi, Junjun Ni*, Tom Sizmur, Ankit Garg*, Sreedeep Sekharan

Name: Suriya Prakash Ganesan
Title: Master's student
Affiliation: Institute of Civil Engineering, Qingdao University of Technology, China
Department of Civil and Environmental Engineering, Shantou University, China
Address: Institute of Civil Engineering, Qingdao University of Technology, China
E-mail: suriyaganesan1075@gmail.com

Name: Sanandam Bordoloi
Title: Post-Doctoral fellow
Affiliation: Department of Civil and Environmental Engineering, Hong Kong University of Science and Technology, China
Address: Department of Civil and Environmental Engineering, Hong Kong University of Science and Technology, China
E-mail: sanandam@ust.hk

Name: Dr Junjun Ni* (Corresponding author)
Title: Visiting Assistant Professor
Affiliation: Department of Civil and Environmental Engineering, Hong Kong University of Science and Technology, China
Address: Department of Civil and Environmental Engineering, Hong Kong University of Science and Technology, China
E-mail: cenijj@ust.hk

Name: Dr Tom Sizmur
Title: Associate Professor
Affiliation: Department of Geography and Environmental Science, University of Reading, United Kingdom
Address: Department of Geography and Environmental Science, University of Reading, United Kingdom
E-mail: t.sizmur@reading.ac.uk

Name: Dr Ankit Garg* (corresponding author)
Title: Associate Professor
Affiliation: Department of Civil and Environmental Engineering, Shantou University, China
Address: Department of Civil and Environmental Engineering, Shantou University, China
E-mail: ankit@stu.edu.cn

Name: Dr. Sreedeep S
Title: Professor
Affiliation: Department of Civil Engineering, Indian Institute of Technology Guwahati, India.
Address: Department of Civil Engineering, Indian Institute of Technology Guwahati, India
E-mail: srees@iitg.ac.in

Abstract

Biochar produced from the pyrolysis of plant based feedstock has been advocated as an alternative soil amendment for landfill cover. Previous literature indicated that the pyrolysis temperature influences the intra-pore distribution and surface functional groups (especially hydroxyl groups), resulting in "love-hate relationship" of the biochar amended soil (BAS) with water. From the purview of geotechnical engineering, the effect of pyrolysis temperature on geotechnical properties are rarely investigated. In total, three biochar rates (0, 5 and 10%) were considered for a set of geotechnical experiments in sand clay mixture soil with biochar produced at 350 ℃ and 550 ℃. Test results show that biochar addition in soil, in general regardless of pyrolysis temperature, increased the optimum moisture content (OMC), plasticity index, soil water retention characteristics (SWRC) and decreased the maximum dry density (MDD), shear strength parameters (cohesion, friction), erosion rates. Whilst comparing the pyrolysis temperature effects on two biochar amended soils, only marginal effects (in terms of magnitude) on SWRC were observed. The most significant decrease of MDD (or increase of OMC) for 5% (w/w) and 10% (w/w) biochar additions occurred at pyrolysis temperatures of 550 ℃ and 350 ℃, respectively. In addition, biochar produced at lower pyrolysis temperature (350 ^{0}C) was more effective in reducing cracks and enhancing shrinkage area ratio. 10% biochar addition with pyrolysis temperature of 350 ^{0}C was the optimum combination in resisting soil erosion. The study provides evidence that the geotechnical properties of biochar amended soils for landfill cover soil applications could be tailor made by controlling the pyrolysis temperature.

Keywords: cedar wood biochar, hydro-mechanical properties, landfill liner applications, pyrolysis temperature

Notation

CW	Cedar Wood
BAS	Biochar Amended Soil
OMC	Optimum Moisture Content
MDD	Maximum Dry Density
CIF	Crack Intensity Factor
SAR	Shrinkage Area Ratio
SWRC	Soil Water Retention Curve

Statement of Novelty

In this paper, biochars (pyrolyzed from cedar wood feedstock) produced from two different pyrolysis temperatures were amended with soil and examined for geotechnical properties in landfill applications. The previous studies although reported the biochar material impact on soil properties, the influence of pyrolysis temperature in the context of geotechnical assessment has been rarely investigated. This study emphasizes the effect of pyrolysis temperature on various geotechnical properties to better understand the effective utilization of biochar in landfill applications

Introduction

Bio-based soil amendment materials have gained traction in the past decade [**1, 2**]. Among these bio-based amendments, biochar has been rediscovered as a sustainable soil amendment material [**3, 4**]. Biochar is a carbonaceous porous material obtained from thermal degradation of plant-based lignocellulose material under limited supply of oxygen and elevated temperatures termed as pyrolysis [**5, 6**]. The conversion of waste ligno-cellulose material into biochar helps in carbon sequestration and has been extensively used in agricultural practices [**7**]. Recently, soil amended with biochar was advocated as a promising final landfill cover material, as it suitably alters the physical [**8, 9**], hydraulic [**10, 11**], mechanical [**12, 13**] and biological [**14**] properties of the soil. Biochar addition in soil was found to alter the physical properties such as porosity, saturated hydraulic conductivity, surface area, crack potential and soil water retention characteristics (SWRC) [**15-17**]. Those changes in soil physical properties may promote the growth of vegetation, which affects the soil hydrological responses and stability of earthen infrastructures [**18-21**]. The soil mechanical properties such as shear strength, erosion potential and liquefaction potential were also reported to be altered by biochar [**22, 23**]. These variations in geotechnical properties for biochar amended soil (BAS) is majorly attributed to biochar gradation, intra-pores of biochar and surface functional groups.

From the purview of geotechnical engineering, the production conditions (e.g. pyrolysis temperature) and its consequent effect on geotechnical properties has rarely been investigated. It is important to understand these relationships because the pyrolysis temperature plays a pivotal role in determining the biochar particle size, its inherent intra-pore distribution and surface functional groups (whether hydrophilic or hydrophobic) [**24**]. From a material science perspective, the effect of pyrolysis temperatures and feedstock types on chemical, morphological and physical characteristics has been well documented [**25-27**]. Studies clearly indicated that the feedstock types affect the biochar yield, elemental compositions and other soil properties such as porosity and bulk density [**28**]. This is due to variation in cellulose, hemicellulose and lignin for different plant-based biomass [**29**]. In addition, the “love hate relationship” of soil-biochar composite and water is influenced by the variations of surface functional groups and morphology at different pyrolysis temperatures. In biochar, where a broad spectrum of hydroxyl group (-OH) found at the surface of the biochar, determines the hydrophilic nature of the biochar. Previous studies reported that the hydrophilic nature of the biochar increases its affinity towards water [**30, 31**]. In the contrary, the biochar produced at higher temperature can increase the number of intrapores (mesopores). The increased intrapores have the ability to store water but possess less affinity towards water due to the hydrophobic nature of the biochar (less pronounced hydroxyl band). As functional groups and biochar intra-pores influence the granular arrangement, water retention and strength characteristics of BAS, it is imperative that the geotechnical properties of the composite with biochar produced at different temperatures need to be explored. This exploration will help geotechnical practitioners have a better understanding on the use of biochar which might pave way to a new direction for classification system for biochar, as is the case for fly ash [**32**].

The overarching aim of this work is to provide an elementary understanding of the influence of pyrolysis temperature on the geotechnical properties of BAS. Cedar wood biochar obtained after in-house pyrolysis at 350 ℃ and 550 ℃ was mixed with a silty sand soil at 0%, 5% and 10% (w/w). The composites prepared were measured for their compaction characteristics, Atterberg limits, shrinkage and crack area ratio, shear strength, erosion potential and SWRC. The microstructure of biochar and surface functional groups were analyzed beforehand to facilitate the interpretation of these measured parameters.

Materials and Methods

Soil and biochar characteristics

An un-amended bare soil and four cedar wood biochar amended soil designated as CW-T-BP (refer Table **1**), were analyzed in the current study. The soil was classified as sand clay mixture (SC) according to Unified Soil Classification System [**33**]. The soil consists of 50% sand (coarse sand-19%, medium sand-16% and fine sand-16%), 19% silt and 30% clay particles. The Atterberg limits, compaction characteristics and specific gravity are tabulated in Table **2**. This type of soil has been extensively used as a cover material in landfill liner in countries, such as India, Hong Kong and United States [**34-37**].

The produced biochars were tested for the surface functional groups and significant changes of hydrophilic groups were observed in the biochars pyrolyzed at 350 ℃ (CW-350) and 550 ℃ (CW-550). CW-350 contained un-pyrolyzed hydrophilic surfaces and functional groups, while CW-550 was fully pyrolyzed and aromatic in nature. These two biochars were selected for further investigation and, since they were broadly representative of low temperature (incomplete) pyrolysis and high temperature (complete) pyrolysis as reported in literature for the selected feedstock [38]. The chemical properties of feedstock and the corresponding biochars are presented summarized in Table 3.

Surface properties of biochar

The morphology of the two produced biochars were analyzed using Field Emission Scanning Electron Microscopy (FE-SEM). Figure **1** clearly showcased the contrasting morphology of the two biochars wherein a high density of intra-pores is observed in case of CW-550. This observation is expected due to the thermal degradation of relatively simple biopolymers (cellulose and hemicellulose), which degrades faster than complex lignin biopolymers [**15, 39**]. At both magnifications (200X and 1000X), CW-550 reveals a honeycomb intra-pore structure on the entirety of its surface, which was not seen at CW-350. This honeycomb structure is expected as lignin engulfs the cellulose and hemicellulose biopolymers in a similar structural arrangement [**40**]. Figure 2 helps us to understand the surface functional groups of the two produced biochars by analyzing the infrared spectrum of absorption using Fourier Transformation Infra-Red (FTIR) spectroscopy. It is clearly visible that the major hydrophilic functional group i.e. hydroxyl disappears at CW-550 indicated by the apparent reduction of peaks at wavelengths near 3500 cm^{-1} (Fig. **2**). In general, the peaks for most of the functional groups are less pronounced for CW-350, compared to CW-550, indicating that the water holding capacity of the biochar would be reduced with higher pyrolysis temperatures.

Experimental setup and procedure

The shrinkage area ratio (SAR) and crack intensity factor (CIF), which gives an indication of the shrinkage and desiccation potential of soil was measured using image analysis [**36, 41, 42**]. For CIF and SAR experiments, all the soil samples were prepared at liquid limit state in a cylindrical mould (20 cm in diameter) and the samples were allowed to dry naturally at room temperature. At regular interval of 60 minutes, images of the surface area and the corresponding water content in the soil have been monitored. The CIF and SAR values were calculated from the image analysis of the obtained pictures.

For erosion assessment, the BAS samples are statically compacted within the mold having the dimensions of 2.5 cm diameter and 5 cm length, respectively. A 7 mm diameter opening is drilled at the center of the sample along the axis. The size of the hole was based on the consideration that the higher flow rates require a bigger hole to initiate erosion and a small hole may cause significant re-deposition of eroded particles on its walls [**43**]. Drilled samples were installed in pinhole setup and was subjected to different increasing continuous flowrates. The eroded particles were collected by passing the eroded effluent through Whatman filter paper (Fig. 5e). The eroded mass was estimated by oven drying method. The shear stress and erosion rate for a specific flow rate was estimated. The corresponding critical shear stress and erodibility coefficient were estimated for every soil state as done previously by Kumar et al. [**23**]

The shear strength parameters such as cohesion and friction angle were measured using the direct shear apparatus. The soil samples were prepared in a shear box of dimension 60 mm*60 mm*50 mm at maximum density obtained from the compaction characteristics. The instrument provides the shear stress value for the applied normal stress. The shear strength parameters of cohesion and friction angle were obtained from the shear stress vs normal stress plots. The soil water retention curve was measured using WP4C dew point potentiometer, which gives the indirect measurement of soil suction using the kelvin equation considering the humidity of the air above soil sample [**44**]. The gravimetric water content of the soil sample is measured followed by the suction measurement. The soil samples were prepared at maximum dry density state. All the experiments were repeated three times at a minimum in order to minimize errors and ascertain the variability.

Results and Discussion

Index properties and compaction state of biochar amended soil

The Atterberg limits (liquid limit, plastic limit and shrinkage limit) for bare soil and BAS are reported in Table **2**. There is a significant increase in the liquid limit and plastic limit for BAS at both temperatures (350 ℃ and 550 ℃). This observation is attributed to the higher intra pore spaces (Fig. **1**) which facilitate more water to be stored in the soil voids as well as in the intra-pore voids [**23**]. The plasticity index was also sensitive to the addition of biochar, and was increased at higher application rates and at higher pyrolysis temperatures. Figure **3** shows the compaction curves for bare soil and BAS. The maximum dry density and corresponding optimum moisture content (OMC) for the bare soil were 17 kN/m^3 and 17.2%, respectively. It was seen that after addition of biochar, the dry density decreased to 15.5–13.1 kN/m^3, while the OMC increased to 19.1%-25.2%, depending on the amendment rate and pyrolysis temperature. In 5% biochar addition, the magnitude of MDD decrease and OMC increase was higher at CW-550. This can be explained by very finer particle size of the biochar obtained at 550 ℃ pyrolysis temperature than that at 350 0C. The finer biochar particles at CW-550 increases the specific surface areas [**45**] and reduces the specific gravity of the composite to a greater extent than those at CW-350. Hence the MDD value decreased and OMC increased significantly at CW-550 for 5% biochar amendment rate. However, for 10% biochar addition, the characteristics are reversed, such that the magnitude of MDD decrease and OMC increase was higher at CW-350. Since the amendment rate is high, the finer particles of biochar at CW-550 tightly clogged soil voids during compaction. This mechanism can be substantiated by the surface morphology images portrayed in Fig. **1** and previous report by **[45]**. The tightly packed soil-biochar composite with pore clogging is implausible at CW-350 due to quite coarser nature of biochar obtained at 350 ℃ pyrolysis temperature. Therefore, MDD decrease and OMC increase was found to be higher at CW-350. Based on the above discussion, it can be concluded that biochar particle size has greater influence on compaction characteristics for smaller biochar amendment rate (e.g., 5%). However, for higher amendment rate (e.g., 10%), the compaction characteristics are mainly dominated by pore clogging of fine particles in the composite.

Shrinkage and desiccation potential of biochar amended soil

Figure **4** shows the CIF and SAR variation at different water content for bare soil and BAS. CIF is the ratio of the cracked area at the soil surface to the total area of the soil specimen [**42, 46**]. As water content decreases, the CIF increases from zero up to a certain value and then levels off indicating peak CIF [**36, 47**]. The peak CIF decreases with respect to bare soil by almost 73% for both CW-350-5% and CW-350-10%. For CW-550-5% and CW-550-10%, the peak CIF decreases up to 56% and 66%, respectively. At CW-350, as the hydroxyl groups are abundant (seen in the FTIR spectra) and the water present in the resulting BAS naturally results in less cracks. On the other hand, the lesser abundance of hydroxyl groups on the surface of CW-550 means that it retains less water and thus has a higher CIF at both amendment rates compared to CW-350. The SAR indicates the ratio of shrinked area to the initial cross-sectional area of soil [**48**] The BS shrinks to

74% of original area whereas CW-350-5% and CW-350-10% shrinks to 86% to 89% of original area relatively at the end of drying. The CW-550-5% and CW-550-10% shrinks up to 75% to 79% of original area, thus showing that CW-350 has better shrinkage mitigation overall (similar to CIF response).

Shear strength and erodibility parameters of biochar amended soil

Figure **5** presents the shear stress versus normal stress response for all soil samples and their respective shear parameters (cohesion (c) and angle of friction (ϕ)). It can be seen that cohesion of BAS decreases with respect to bare soil. The ϕ increases with addition of biochar for both BAS prepared at 350 ℃ and 550 ℃. In the context of amendment rates, for the BAS, the composite prepared at 550 ℃ showed less cohesion with respect to 350 ℃ which can be explained by the absence of hydrophilic (-OH) groups. At 350 ℃, with an increase in biochar amendment rate, the cohesion increases due to more abundant (-OH) groups. The same is not observed for BAS with CW-550 since cohesion is lower at the higher application rates. At biochar amendment rate 10%, CW-550 has a higher percentage of finer particles that CW-350. The increased fine particles can reduce the contact friction between coarse grains and hence decrease the shear resistance [**49**]. That is why at lower normal stress (50 kPa), CW-550 has much lower shear strength than CW-350. However, with the increase of normal stress to 150 kPa, stress-induced particle rearrangement and clogging of soil pores by finer biochar particles become more significant in CW-550 (Fig. **1**). The increase of pore clogging and hence soil density under higher stress in CW-550 causes the interlocking between particles and hence the tendency to soil dilatancy [**50**], resulting in a higher shear strength.

Figure **6** shows the variation of erosion rate with shear stress for bare soil and BAS for three different compaction states (i.e. OMC-5%, OMC and OMC+5%). It was seen that an increase in moisture resulted in decrease in erosion rate for both BS and BAS, which is attributed to apparent cohesive force between soil particles in the presence of water [**51**] and the particle orientation change from flocculated to dispersed [**52**]. Runoff water can easily erode the flocculated particles in dry side, as there is edge-to-face interaction. On the other hand, flow happens along the particle surface in dispersed orientation (wet side) producing relatively less drag [**53**]. The effect of different pyrolysis temperature was evident in the erosion response for BAS constituted by hydrophilic CW-350-5% and CW-350-10%, showing lower erosion with respect to

CW-550-5% and CW-550-10%, at all compaction states. Furthermore, the erosion rate decreases with increased amendment rates for both CW-350 and CW-550.

Soil water retention of biochar amended soil

Figure **7** presents the soil water retention response of bare soil and BAS. It was observed that inclusion of both CW-350 and CW-550 in soil increased the water retention capacity of the soil. Regardless of the biochar amendment rate and pyrolysis temperature, all BAS gave a similar SWR response. This response of BAS was also observed by Wong et al. [**54**] for compacted Kaolinite soil (at 0.9 degree of compaction) amended with peanut-shell biochar (Fig. **7**). Thus, it can be inferred that at high suction (beyond 1000 kPa), the effect of different functional groups and intra-pore volume of biochar does not significantly affect the SWR.

Conclusions

This study explored the effects of biochar pyrolyzed at 350 ℃ and 550 ℃ applied to a silty sand at 5% and 10% (w/w) on the geotechnical properties of the amended soil. The microstructure of produced biochar and its surface functional groups revealed that the intra-pores increase, and surface functional group were lower for biochar produced at higher temperature. There is contrasting hydrophobic and hydrophilic characteristics of biochar as pyrolysis temperature increases, due to decrease in -OH groups and higher intra-pore volume, respectively. The pyrolysis temperature played a major role by altering the basic compaction characteristics (increase in OMC and decrease in dry density due to its porous nature) as reported in previous studies. Whilst analyzing the major objective, biochar pyrolyzed at lower temperature (CW-350) mitigates better in cracking and shrinkage potential than the higher temperature residues (CW-550). This is mainly due to the hydrophilic nature of CW-350, which helps at retaining water in the soil-biochar matrix. However, the same advantage contradicts the shear strength properties with decrease in cohesion irrespective of the amendment rates. On the other hand, the soil water retention curves also shows better response when compared with the bare soil, due to the obvious water retention in the intrapores of the biochar. Thus, the biochar produced at lower temperatures might act better in the landfill applications after plant establishment (for strength increase) of the cover surface considering the aspects of energy reduction and cost intensiveness. Besides, the adverse effects of pyrolysis temperature with biochar obtained from different feedstocks and the effect of pyrolysis temperature on leaching potential of BAS should be studied in future.

Acknowledgments

The authors would like to acknowledge Shantou University Scientific Research Fund (NTF17007) for the support.

References

1. Liang S, Han Y, Wei L, McDonald AG (2014) Production and characterization of bio-oil and bio-char from pyrolysis of potato peel wastes. Biomass Conv Bioref 5:237-246. https://doi.org/10.1007/s13399-014-0130-x
2. Machineni L (2019) Lignocellulosic biofuel production: review of alternatives. Biomass Conv Bioref. https://doi.org/10.1007/s13399-019-00445-x
3. Shalini SS, Palanivelu K, Ramachandran A, Raghavan V (2020) Biochar from biomass waste as a renewable carbon material for climate change mitigation in reducing greenhouse gas emissions—a review. Biomass Conv Bioref https://doi.org/10.1007/s13399-020-00604-5
4. Singh R, Srivastava P, Singh P, Sharma AK, Singh H, Raghubanshi AS (2019) Impact of rice-husk ash on the soil biophysical and agronomic parameters of wheat crop under a dry tropical ecosystem. Ecol Indic 105:505-515. https://doi.org/10.1016/j.ecolind.2018.04.043
5. Liu R, Liu G, Yousaf B, Abbas Q (2018) Operating conditions-induced changes in product yield and characteristics during thermal-conversion of peanut shell to biochar in relation to economic analysis. J Clean Prod 193:479-490. https://doi.org/10.1016/j.jclepro.2018.05.034
6. Yang S, Li B, Zheng J, Kankala RK (2018) Biomass-to-Methanol by dual-stage entrained flow gasification: Design and techno-economic analysis based on system modeling. J Clean Prod 205:364-374. https://doi.org/10.1016/j.jclepro.2018.09.043

7. Jeffery S, Verheijen FG, Van der Velde M, Bastos AC (2011) A quantitative review of the effects of biochar application to soils on crop productivity using meta-analysis. Agr Ecosyst Environ 144(1):175-187. https://doi.org/10.1016/j.agee.2011.08.015
8. Ulyett J, Sakrabani R, Kibblewhite M, Hann M (2014) Impact of biochar addition on water retention, nitrification and carbon dioxide evolution from two sandy loam soils. Eur J Soil Sci 65(1):96-104. https://doi.org/10.1111/ejss.12081
9. Abel S, Peters A, Trinks S, Schonsky H, Facklam M, Wessolek G (2013) Impact of biochar and hydrochar addition on water retention and water repellency of sandy soil. Geoderma 202:183-191. https://doi.org/10.1016/j.geoderma.2013.03.003
10. Wong JTF, Chen Z, Chen X, Ng CWW, Wong MH (2017) Soil-water retention behavior of compacted biochar-amended clay: a novel landfill final cover material. J Soil Sediment 17(3):590-598. https://doi.org/10.1007/s11368-016-1401-x
11. Yaghoubi P, Reddy KR (2011) Characteristics of biochar-amended soil cover for landfill gas mitigation. In Pan-Am CGS Geotechnical Conference.
12. Chen XW, Wong JTF, Ng CWW, Wong MH (2016) Feasibility of biochar application on a landfill final cover—a review on balancing ecology and shallow slope stability. Environ Sci Pollut Res 23(8):7111-7125. https://doi.org/10.1007/s11356-015-5520-5
13. Das O, Sarmah AK, Bhattacharyya D (2016) Bio composites from waste derived biochars: mechanical, thermal, chemical, and morphological properties. Waste Manag 49:560-570. https://doi.org/10.1016/j.wasman.2015.12.007
14. Swagathnath G, Rangabhashiyam S, Murugan S, Balasubramanian P (2019) Influence of biochar application on growth of *Oryza sativa* and its associated soil microbial ecology. Biomass Convers Bioref 9:341-352. https://doi.org/10.1007/s13399-018-0365-z
15. Pardo GS, Sarmah AK, Orense RP (2018) Mechanism of improvement of biochar on shear strength and liquefaction resistance of sand. Geotechnique 69(6):471-480. https://doi.org/10.1680/jgeot.17.P.040
16. Ni JJ, Chen XW, Ng CWW, Guo HW (2018) Effects of biochar on water retention and matric suction of vegetated soil. Geotech Lett 8(2):124-129. https://doi.org/10.1680/jgele.17.00180

17. Ni JJ, Bordoloi S, Shao W, Garg A, Xu G, Sarmah AK (2020) Two-year evaluation of hydraulic properties of biochar-amended vegetated soil for application in landfill cover system. Sci Total Environ 712:136486. https://doi.org/10.1016/j.scitotenv.2019.136486
18. Ng CWW, Ni JJ, Leung AK (2019a) Effects of plant growth and spacing on soil hydrological changes: A field study. Géotechnique. https://doi.org/10.1680/ jgeot.18.P.207
19. Ng CWW, Ni JJ, Leung AK (2019b) Plant-Soil Slope Interaction. Taylor & Francis. ISBN 978-1-138-19755-8. 8. 206p. 1st Edition: 2 Aug 2019.
20. Ni JJ, Leung AK, Ng CWW (2019a) Modelling effects of root growth and decay on soil water retention and permeability. Can Geotech J 56(7): 1049-1055. https://doi.org/ 10.1139/cgj-2018-0402
21. Ni JJ, Leung AK, & Ng CWW (2019b) Unsaturated hydraulic properties of vegetated soil under single and mixed planting conditions. Géotechnique 69(6): 554-559. https://doi.org/ 10.1680/jgeot.17.T.044
22. Reddy KR, Yaghoubi P, Yukselen-Aksoy Y (2015) Effects of biochar amendment on geotechnical properties of landfill cover soil. Waste Manag. Res 33(6):524-532. 10.1177/0734242X15580192
23. Kumar H, Ganesan SP, Bordoloi S, Sreedeep S, Lin P, Mei G, Garg A, Sarmah AK (2019) Erodibility assessment of compacted biochar amended soil for geo-environmental applications. Sci Total Environ 672:698-707. https://doi.org/10.1016/j.scitotenv. 2019.03.417
24. Liu Z, Dugan B, Masiello CA, Gonnermann HM (2017) Biochar particle size, shape, and porosity act together to influence soil water properties. PloS One 12(6):e0179079. https://doi.org/10.1371/journal.pone.0179079
25. Angin D, Şensoz S (2014) Effect of pyrolysis temperature on chemical and surface properties of biochar of rapeseed (*Brassica napus L.*). Int J Phytoremediat 16(7-8):684-693. https://doi.org/10.1080/15226514.2013.856842
26. Sun Y, Gao B, Yao Y, Fang J, Zhang M, Zhou Y, Chen H, Yang L (2014) Effects of feedstock type, production method, and pyrolysis temperature on biochar and hydrochar properties. Chem Eng J 240:574-578. https://doi.org/10.1016/j.cej.2013.10.081

27. Guizani C, Jeguirim M, Valin S, Limousy L, Salvador S (2017) Biomass chars: The effects of pyrolysis conditions on their morphology, structure, chemical properties and reactivity. Energies 10(6):796. https://doi.org/10.3390/en10060796
28. Alburquerque JA, Calero JM, Barrón V, Torrent J, Campillo MC, Gallardo A, Villar R (2014) Effects of biochars produced from different feedstocks on soil properties and sunflower growth. J Plant Nutr Soil Sci 177(1):16-25. https://doi.org/10.1002/jpln.201200652
29. Bordoloi S, Garg A, Sekharan S (2017) A review of physio-biochemical properties of natural fibers and their application in soil reinforcement. Adv Civ Eng Mater 6(1):323-359. https://doi.org/10.1520/ACEM20160076
30. Das O, Sarmah AK (2015) The love–hate relationship of pyrolysis biochar and water: a perspective. Sci Total Environ 512:682-685. https://doi.org/10.1016/j.scitotenv.2015.01.061
31. Gray M, Johnson MG, Dragila MI, Kleber M (2014) Water uptake in biochar: The roles of porosity and hydrophobicity. Biomass Bioenerg 61:196-205. https://doi.org/10.1016/j.biombioe.2013.12.010
32. Roy WR, Thiery RG, Schuller RM, Suloway JJ (1981) Coal fly ash: a review of the literature and proposed classification system with emphasis on environmental impacts. Environ Geol 96.
33. ASTM D2487 (2017) Standard Practice for Classification of Soils for Engineering Purpose (Unified Soil Classification System). ASTM International, West Conshohocken, PA.
34. Sadasivam BY, Reddy KR (2015) Adsorption and transport of methane in landfill cover soil amended with waste-wood biochars. J Environ Manag 158:11-23. https://doi.org/10.1016/j.jenvman.2015.04.032
35. Ng CWW, Chen R, Coo JL, Jian L, Ni JJ, Chen Y, Zhan L, Guo H, Bangwen L (2018) A novel vegetated three-layer landfill cover system using recycled construction wastes without geomembrane. Can Geotech J 56(12):1863-1875. https://doi.org/10.1139/cgj-2017-0728
36. Bordoloi S, Garg A, Sreedeep S, Lin P, Mei G (2018) Investigation of cracking and water availability of soil-biochar composite synthesized from invasive weed water hyacinth. Bioresour Technol 263:665-677. https://doi.org/10.1016/j.biortech.2018.05.011

37. Sheikh J, Bordoloi S, Yamsani S, Sreedeep S, Rakesh RR, Sarmah AK (2019) Long-term hydraulic performance of landfill cover system in extreme humid region: Field monitoring and numerical approach. Sci Total Environ 688:409-423. https://doi.org/10.1016/j.scitotenv.2019.06.213
38. Rodríguez-Vila A, Selwyn-Smith H, Enunwa L, Smail I, Covelo EF, Sizmur T (2018) Predicting Cu and Zn sorption capacity of biochar from feedstock C/N ratio and pyrolysis temperature. Environ Sci Pollut Res 25(8):7730-7739. 10.1007/s11356-017-1047-2
39. Lehmann J, Joseph S (2015) Biochar for environmental management: science, technology and implementation. Routledge.
40. Bordoloi S, Gopal P, Boddu R, Wang Q, Cheng YF, Garg A, Sreedeep S (2019) Soil-biochar-water interactions: role of biochar from Eichhornia crassipes in influencing crack propagation and suction in unsaturated soils. J Clean Prod 210:847-859. https://doi.org/10.1016/j.jclepro.2018.11.051
41. Rasband WS (2011) ImageJ. US National Institutes of Health, Bethesda, Maryland, USA.
42. Yesiller N, Miller, CJ, Inci G, Yaldo K (2000) Desiccation and cracking behavior of three compacted landfill liner soils. Eng Geol 57(1-2):105-121. https://doi.org/10.1016/S0013-7952(00)00022-3
43. Reddi LN, In-Mo L, Bonala MVS (2000) Comparison of Internal and Surface Erosion Using Flow Pump Tests on a Sand-Kaolinite Mixture. Geotech Test J 23(1):116-122. https://doi.org/10.1520/GTJ11129J
44. Simms P, Soleimani S, Mizani S, Daliri F, Dunmola A, Rozina E, Innocent-Bernard T (2017) Cracking, salinity and evaporation in mesoscale experiments on three types of tailings. Environ Geotech 6(1):3-17. https://doi.org/10.1680/jenge.16.00026
45. Liu Z, Dugan B, Masiello CA, Barnes RT, Gallagher ME, Gonnermann H (2016) Impacts of biochar concentration and particle size on hydraulic conductivity and DOC leaching of biochar–sand mixtures. J Hydrol 533: 461-472. https://doi.org/10.1016/j.jhydrol.2015.12.007
46. Liu Z, Dugan B, Masiello CA, Gonnermann HM (2017) Biochar particle size, shape, and porosity act together to influence soil water properties. Plos one 12(6): e0179079. https://doi.org/10.1371 /journal.pone.0179079

47. Li JH, Li L, Chen T, Li DQ (2016) Cracking and vertical preferential flow through landfill clay liners. Eng Geol 206:33-41. https://doi.org/10.1016/j.enggeo.2016.03.006
48. Wan Y, Wu C, Xue Q, Hui X (2019) Effects of plastic contamination on water evaporation and desiccation cracking in soil. Sci Total Environ 654:576-582. https://doi.org/10.1016/j.scitotenv.2018.11.123
49. Carraro JAH, Prezzi M, Salgado R. (2009) Shear strength and stiffness of sands containing plastic or non-plastic fines. J Geotech Geoenviron 135(9): 1167-1178. https://doi.org/10.1061/(ASCE)1090-0241(2009)135:9(1167)
50. Bolton MD (1986) The strength and dilatancy of sands. Geotechnique 36(1): 65-78. https://doi.org/10.1680/geot.1986.36.1.65
51. Chepil WS (1956) Influence of Moisture on Erodibility of Soil by Wind 1. Soil Sci Soc Am J **20**(2):288-292. https://doi.org/10.2136/sssaj1956.03615995002000020033x
52. Lambe TW (1958) The structure of compacted clay. J Soil Mech Found Div 84(2):1-34
53. Grissinger EH (1966) Resistance of selected clay systems to erosion by water. Water Resour Res **2**(1):131-138. https://doi.org/10.1029/WR002i001p00131
54. Wong JTF, Chen Z, Wong AYY, Ng CWW, Wong MH (2018) Effects of biochar on hydraulic conductivity of compacted kaolin clay. Environ Pollut 234:468-472. https://doi.org/10.1016/j.envpol.2017.11.079
55. ASTM D422–63 (2007) Standard Test Method for Particle-size Analysis of Soils. ASTM International, West Conshohocken, PA.
56. ASTM D4318 (2010) Standard Test Methods for Liquid Limit, Plastic Limit and Plasticity Index of Soils. ASTM International, West Conshohocken, PA.
57. ASTM D1557 (2012) Standard test methods for laboratory compaction characteristics of soil using modified effort. ASTM International, West Conshohocken, PA.
58. ASTM D854 (2014) Standard Test Methods for Specific Gravity of Soil Solids by Water Pycnometer. ASTM International, West Conshohocken, PA.
59. ASTM D3080 (2011) Standard test method for direct shear test of soils under consolidated drained conditions. ASTM International, West Conshohocken, PA.

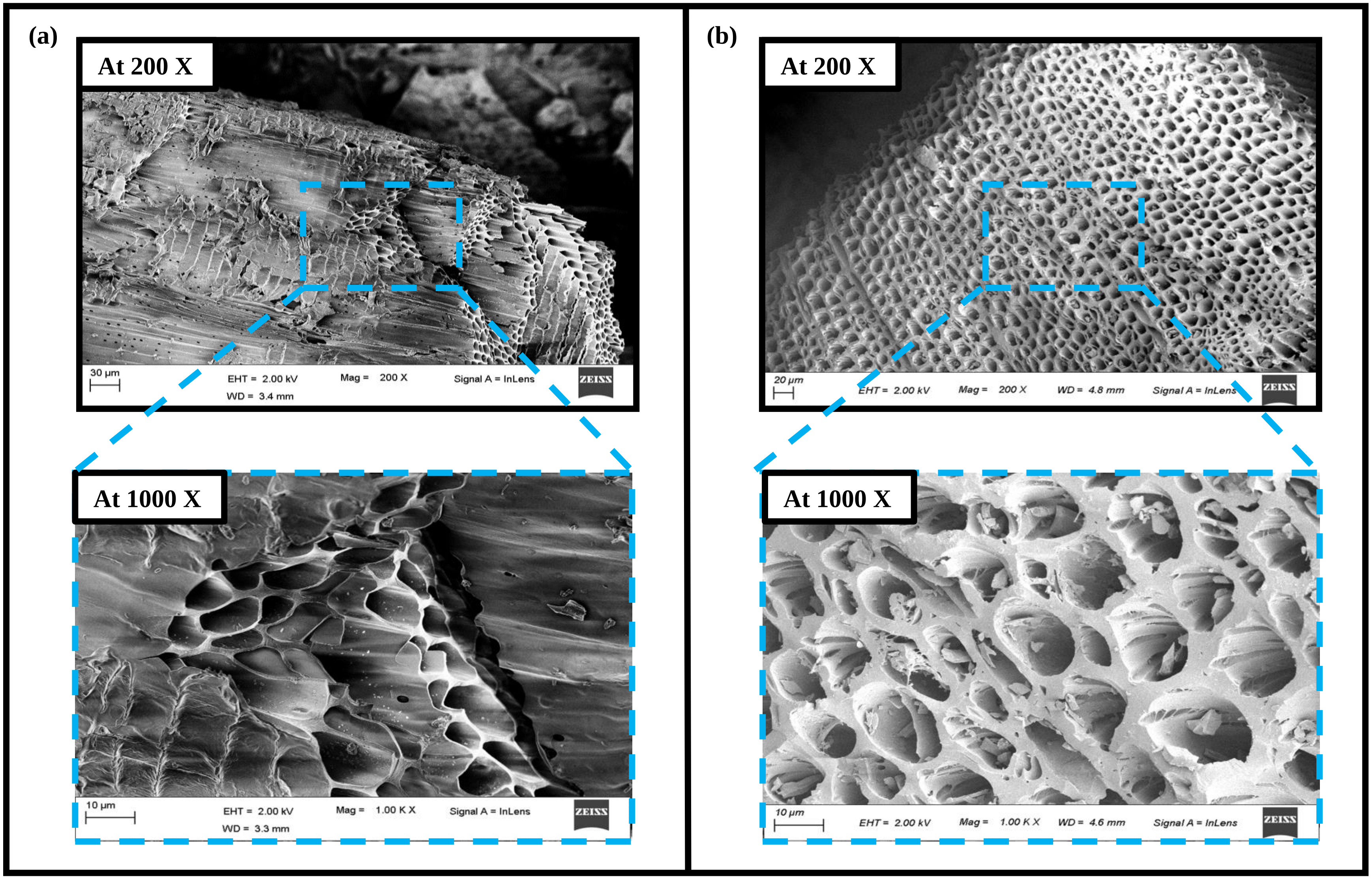

Fig. 1 Surface morphology of cedar wood biochar depicted with FE-SEM images a) 350 °C; b) 550 °C

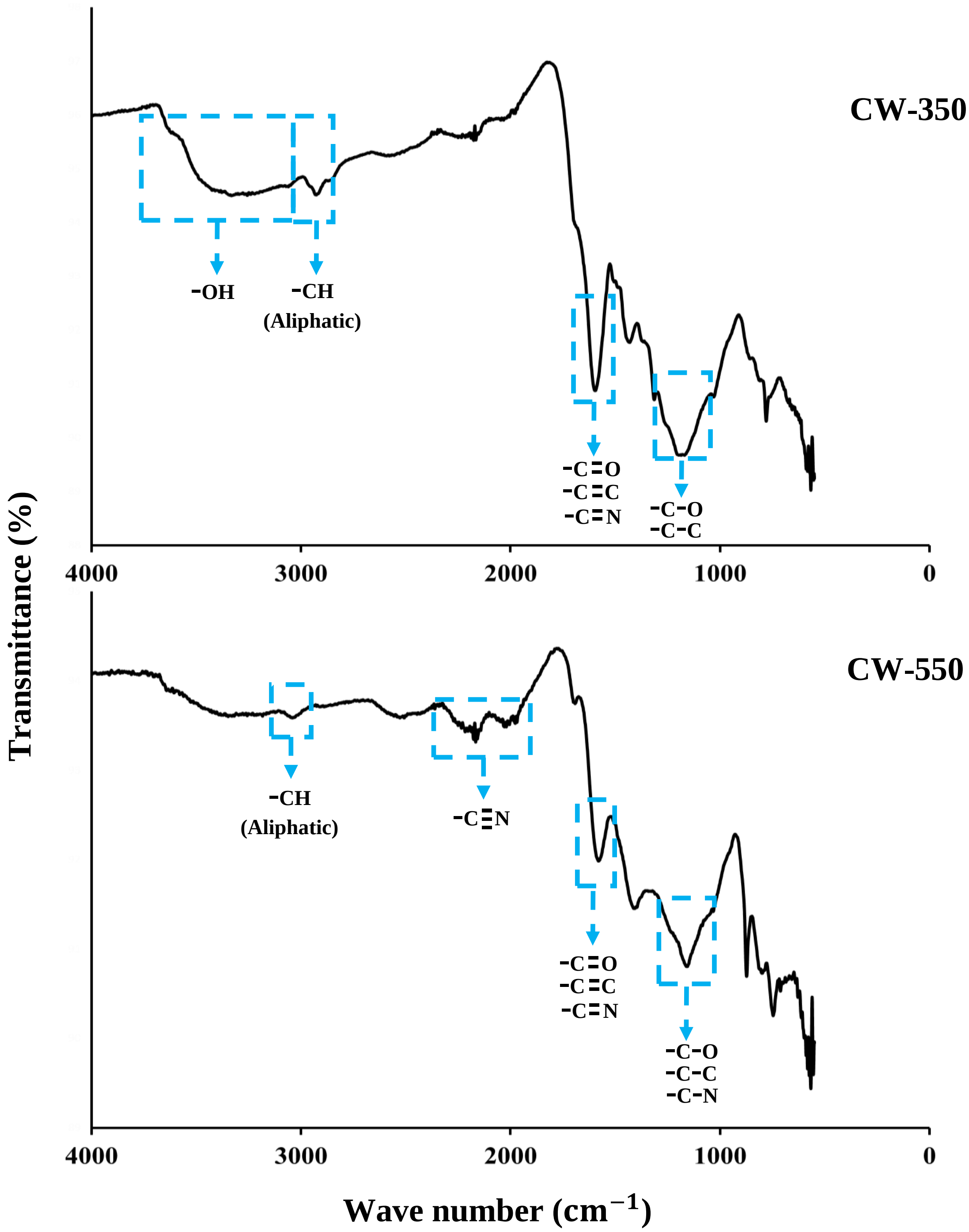

Fig. 2 FTIR results depicting the functional groups of cedar wood biochar at 350 ℃ and 550 ℃

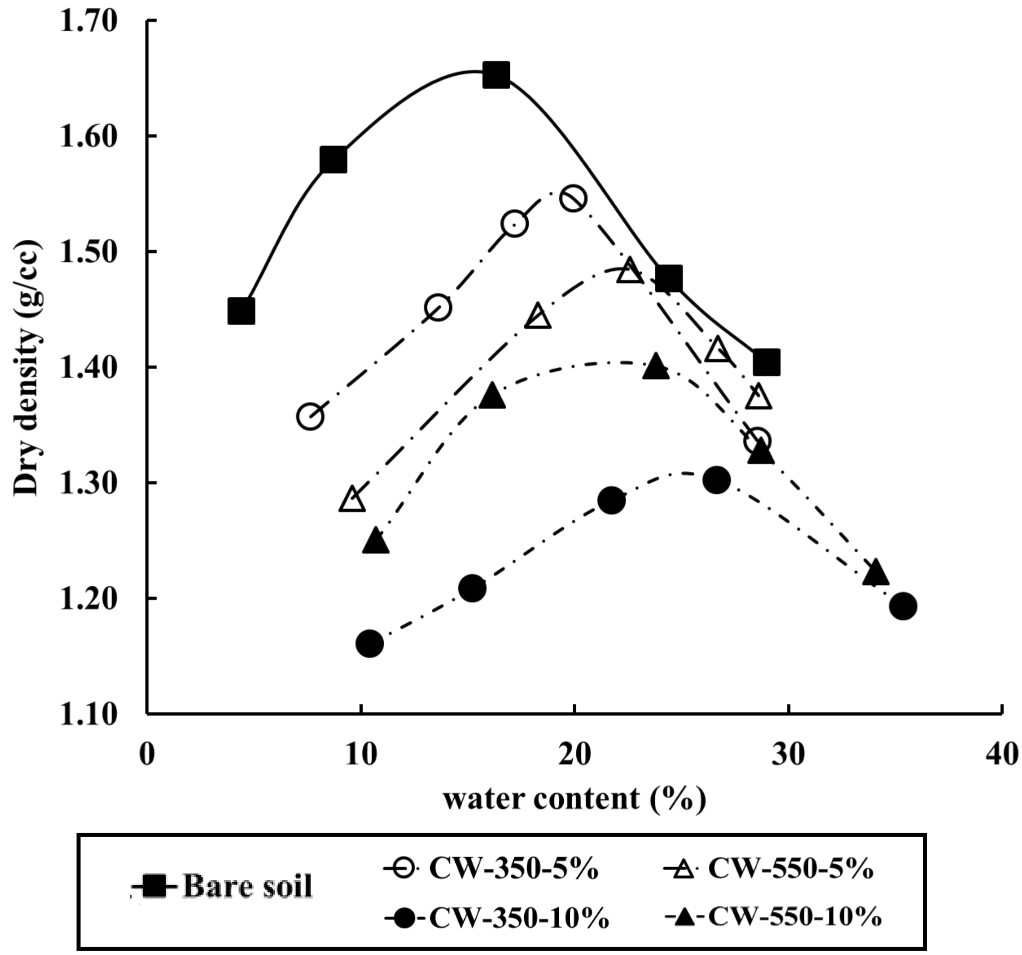

Fig. 3 Compaction curves for bare soil and cedar wood biochar amended soils at 5% and 10%

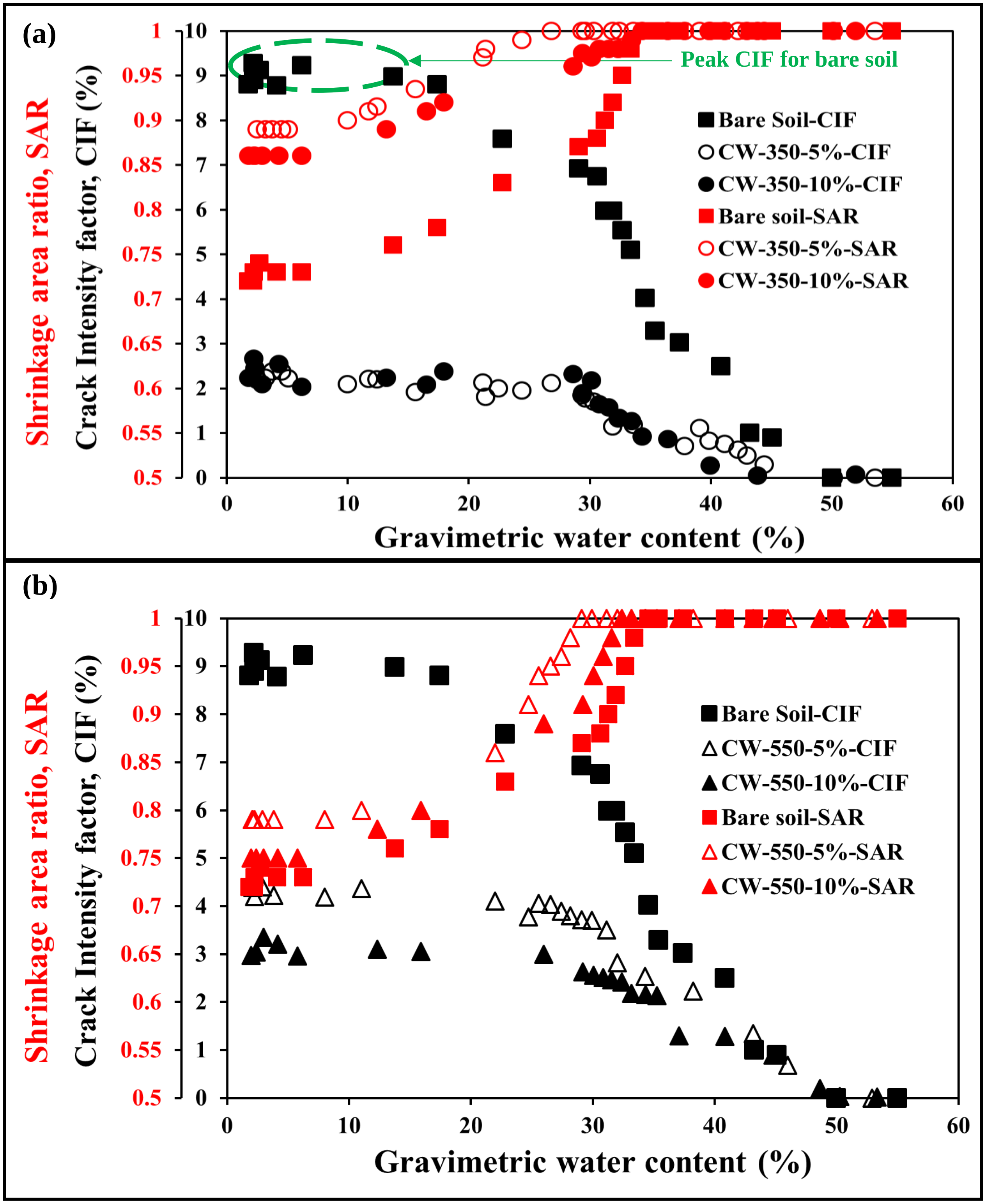

Fig. 4 SAR and CIF variation with moisture content for bare soil and soil-biochar composite produced at (a) 350 ^{0}C and (b) 550 ^{0}C.

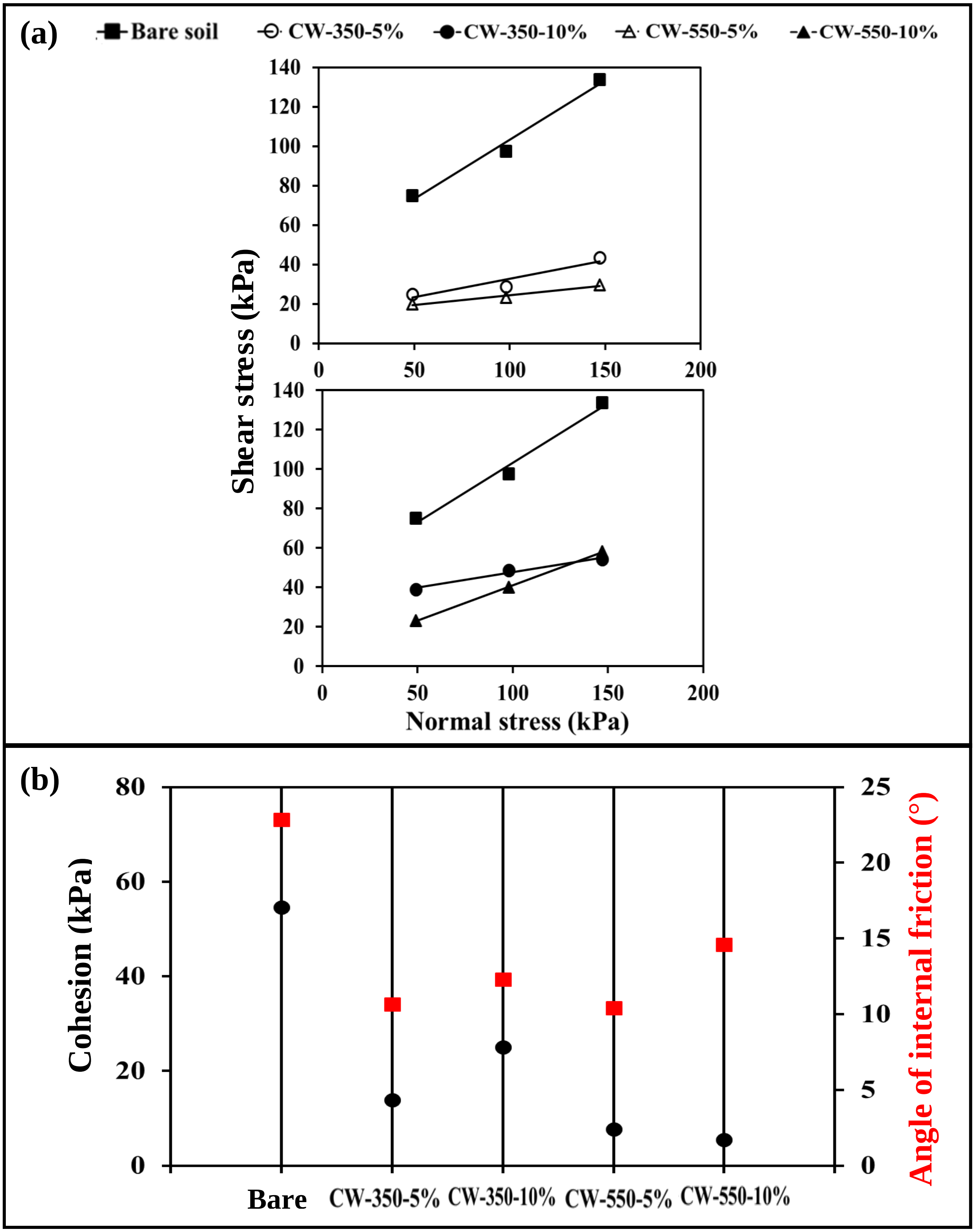

Fig. 5 Direct shear test response for bare soil and biochar amended soil represented as (a) shear stress vs normal stress (b) cohesion and angle of internal friction

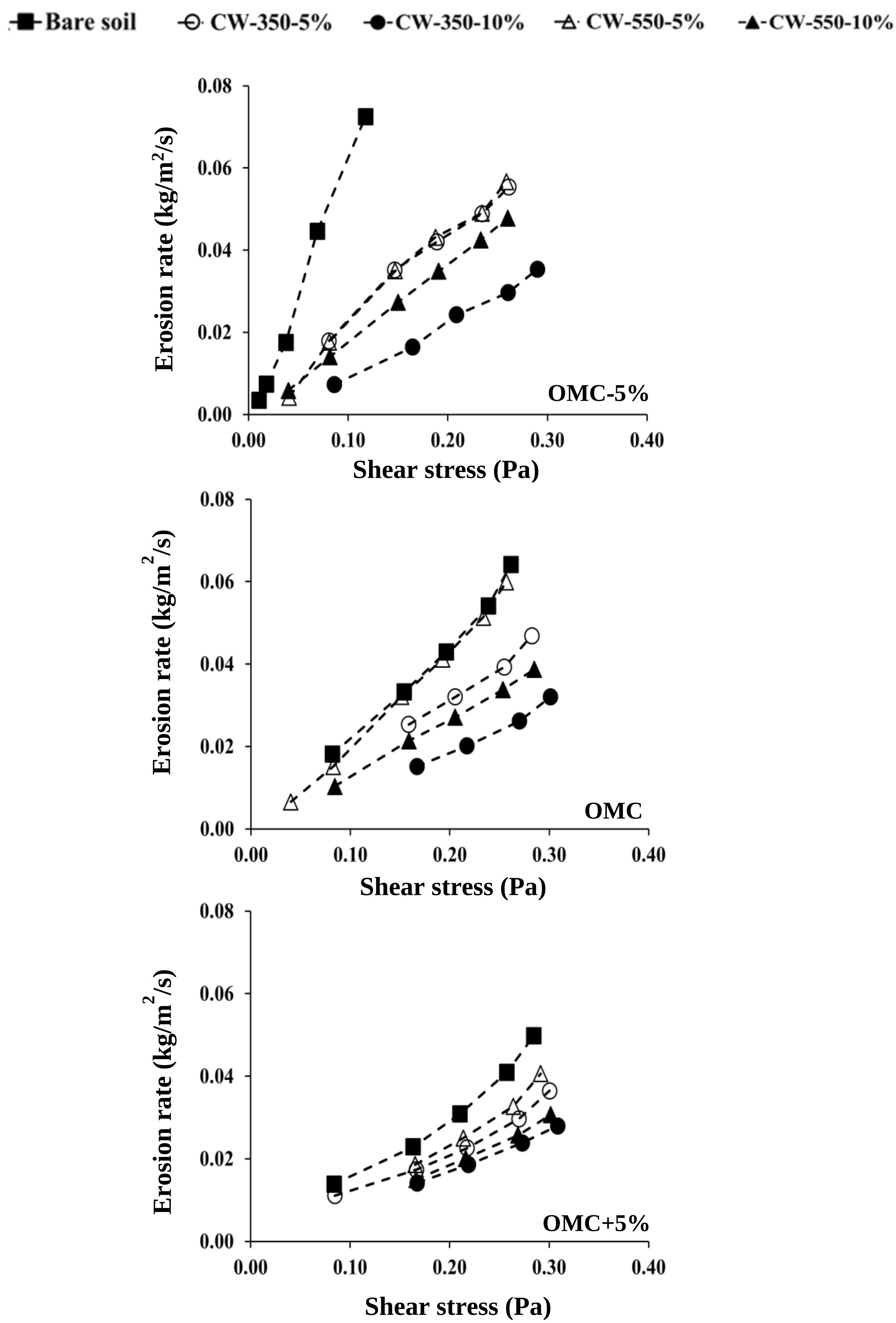

Fig. 6 Pin hole test results representing plots of erosion rate with shear stress

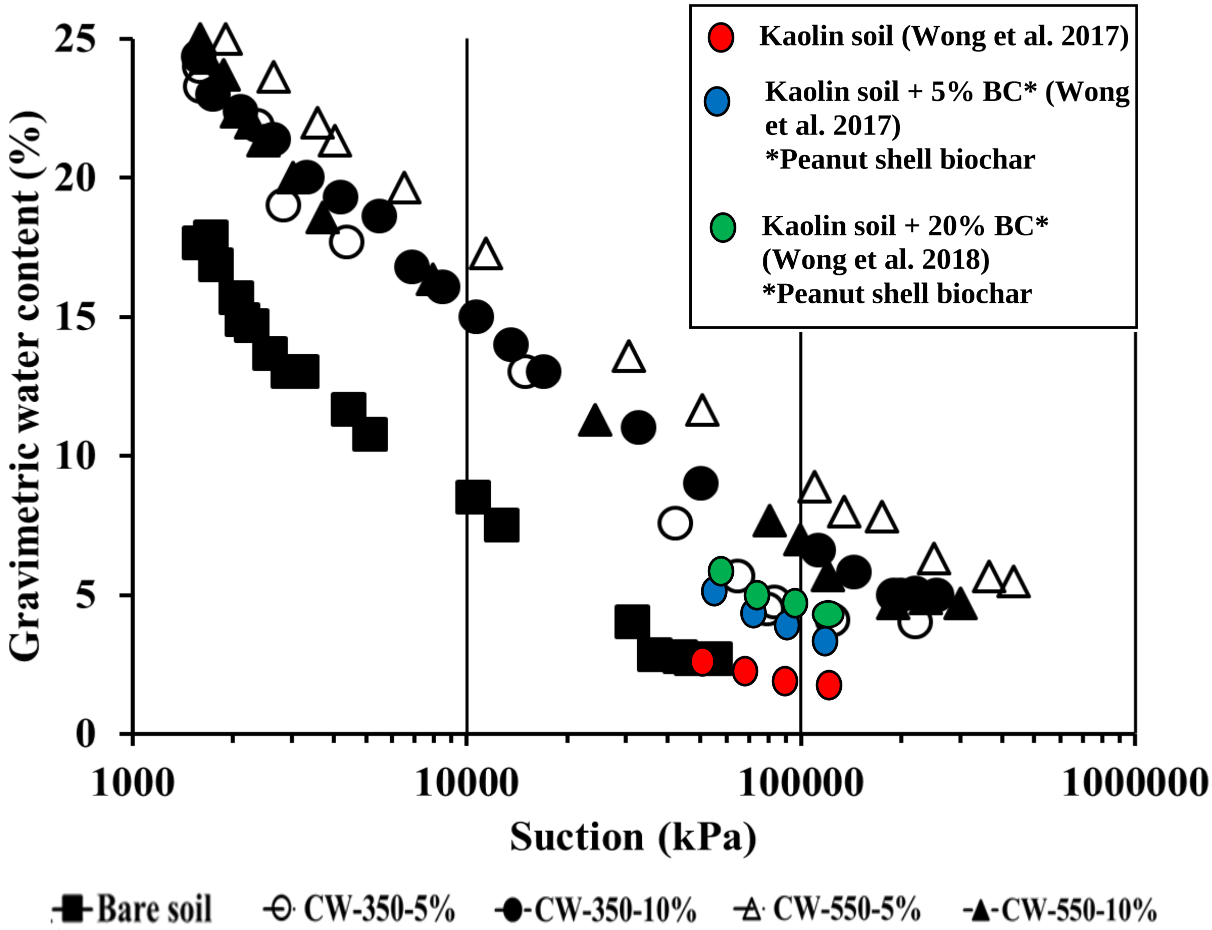

Fig. 7 Soil water retention response for bare soil and biochar amended soil (at 5% and 10%)

Table 1 Designation of materials used to study the geotechnical properties

Test designation	Biochar percentage (%)	Pyrolysis temperature (℃)
BS	NA	NA
CW-350-5%	5	350
CW-350-10%	10	350
CW-550-5%	5	550
CW-550-10%	10	550

Table 2 Physical properties of cedar wood biochar pyrolyzed at 350 ℃ and 550 ℃

Designation	**Consistency limits**				**Compaction parameters**		**Specific gravity of soil and biochar**
	Liquid limit (%)	**Plastic limit (%)**	**Plasticity index**	**Shrinkage limit (%)**	**Optimum Moisture Content (%)**	**Maximum Dry Density (g/cc)**	
	ASTM D 4318-00			ASTM D 4943-18	ASTM D 1557-15		ASTM D 854-14
BS	43.6	25.5	18.1	13.9	17.2	1.70	2.74
CW-350-5%	50.4	30.4	20.1	12.7	19.1	1.55	1.11
CW-350-10%	54.4	33.4	21.0	16.4	25.2	1.31	
CW-550-5%	51.9	29.2	22.7	10.2	22.6	1.49	1.08
CW-550-10%	58.5	30.9	27.5	18.4	24.0	1.4	

Table 3 Pyrolysis condition, chemical properties, and particle size of the produced biochar

Feedstock	Cedar wood	
Pyrolysis temperature	350 ℃	550 ℃
Pyrolysis process	Slow pyrolysis	Slow pyrolysis
Elemental composition		
Carbon (%)	68.71	78.74
Nitrogen (%)	0.41	0.58
Molar ratio		
C: N	168:1	135:1
Ash content (%)	24.1	29.5
CEC (cmol kg^{-1})	21.67	8.38